Exceptional Non-Abelian Topology in Multiband Non-Hermitian Systems

Cui-Xian Guo,[1] Shu Chen,[1,2,3] Kun Ding,[4] and Haiping Hu[1,2,*]

[1]*Beijing National Laboratory for Condensed Matter Physics, Institute of Physics, Chinese Academy of Sciences, Beijing 100190, China*

[2]*School of Physical Sciences, University of Chinese Academy of Sciences, Beijing 100049, China*

[3]*Yangtze River Delta Physics Research Center, Liyang, Jiangsu 213300, China*

[4]*Department of Physics, State Key Laboratory of Surface Physics, and Key Laboratory of Micro and Nano Photonic Structures (Ministry of Education), Fudan University, Shanghai 200438, China*

(Received 31 October 2022; accepted 13 March 2023; published 11 April 2023)

Defective spectral degeneracy, known as exceptional point (EP), lies at the heart of various intriguing phenomena in optics, acoustics, and other nonconservative systems. Despite extensive studies in the past two decades, the *collective* behaviors (e.g., annihilation, coalescence, braiding, etc.) involving multiple exceptional points or lines and their interplay have been rarely understood. Here we put forward a universal non-Abelian conservation rule governing these collective behaviors in generic multiband non-Hermitian systems and uncover several counterintuitive phenomena. We demonstrate that two EPs with opposite charges (even the pairwise created) do not necessarily annihilate, depending on how they approach each other. Furthermore, we unveil that the conservation rule imposes strict constraints on the permissible exceptional-line configurations. It excludes structures like Hopf link yet permits novel staggered rings composed of noncommutative exceptional lines. These intriguing phenomena are illustrated by concrete models which could be readily implemented in platforms like coupled acoustic cavities, optical waveguides, and ring resonators. Our findings lay the cornerstone for a comprehensive understanding of the exceptional non-Abelian topology and shed light on the versatile manipulations and applications based on exceptional degeneracies in nonconservative systems.

DOI: 10.1103/PhysRevLett.130.157201

Exceptional points (EPs) are peculiar spectral singularities induced by non-Hermiticity [1–4]. The past decade has witnessed a myriad of remarkable phenomena and functionalities in optics, photonics, and acoustics pivoted on the non-Hermitian degeneracy [5,6], such as single-mode lasing [7,8], unidirectional transmission or reflection [9–11], enhanced sensing [12–15], and unconventional quantum interference or correlation [16–19]. Unlike Dirac or Weyl point in Hermitian systems, both the eigenenergies and eigenvectors coalesce at an EP. Without symmetry constraints, an EP of second order is stable in two-dimensional (2D) parameter space [20] and extends to exceptional line (EL) in 3D [21–31].

From a "local" perspective, the simplest EP is dictated by a nondiagonalizable two-by-two Hamiltonian whose eigenvalues have a square-root singularity. The EP can be assigned a topological charge [32–34], or discriminant number [20] that signifies the eigenvalue permutation [35,36] and ensures its stability against small perturbations. While most of the aforementioned phenomena are well understood by scrutinizing one single EP, in most generic non-Hermitian settings, multiple exceptional degeneracies may emerge, annihilate, coalesce, and braid with varying system parameters. Thus far, a holistic framework governing these collective behaviors involving multiple EPs (or ELs) and their interplay in multiband systems remains elusive. What new interesting physics is nurtured by multiple EPs or ELs beyond their local descriptions? And are there any "emergent" phenomena intrinsic to multiband systems beyond the two-band case? Addressing these questions not only provides a fundamental understanding of non-Hermitian physics, but also sheds light on the manipulations and functional design of exceptional degeneracies relevant in a wide range of nonconservative systems like coupled ring resonators [37–42], optical waveguides [43–47], acoustic cavities [48–52], or photonic quantum walks [53,54].

In this Letter, we demonstrate that the collective behaviors and parametric evolution of multiple EPs or ELs are governed by a universal non-Abelian conservation rule (NACR). From the rule, we uncover two intriguing and counterintuitive phenomena. Firstly, it is usually taken for granted that two EPs with opposite charges annihilate each other. In stark contrast, we show that an EP pair (even the pairwise created) in multiband non-Hermitian systems does not necessarily annihilate. Their annihilation or coalescence is path dependent and exhibits an "adjacent" effect. Secondly, as stereotyped in the two-band case, either the nodal lines [27,28,55–61] or ELs [21–31] can form any desired configurations (e.g., Hopf link, trefoil knot, etc.). In multiband settings, the NACR puts strict constraints on the permissible configurations and evolution of ELs. For instance, structures like Hopf link composed of non-commutative ELs are forbidden, while novel staggered exceptional rings are allowed. We further propose a three-state system readily realizable in various experimental platforms (e.g., acoustic cavities) to observe these phenomena. We emphasize that these unexpected results are a consequence of the underlying non-Abelian topology and intrinsic to multiband non-Hermitian systems.

Non-Abelian conservation rule (NACR).—We consider a generic N-band non-Hermitian system. The parameter space is punctured by some exceptional degeneracies [EPs (ELs) in 2D (3D)], as sketched in Fig. 1(a). To address their collective behaviors, we investigate the closed paths with a base point $\boldsymbol{P}$ (start and end point) enclosing these degeneracies in the parameter space. Such closed paths are characterized by the fundamental group of the Hamiltonian space X_N [62–68]:

$$\pi_1(\boldsymbol{P}, X_N) = B_N. \tag{1}$$

B_N is the braid group. Thus each path is assigned a braid-valued topological invariant. It describes how the complex eigenenergies evolve along the path. B_N is non-Abelian except for $N = 2$ with $B_2 = \mathbb{Z}$, wherein the braid invariant is the discriminant number [20]. Figure 1(b) depicts a representative eigenlevel braiding along some closed path. A convenient way to obtain the braid invariant is through Artin's word. After sorting the real parts of eigenenergies as $\mathrm{Re}E_1 \leq \mathrm{Re}E_2 \leq \ldots \leq \mathrm{Re}E_N$, the ith level crosses over or under the $(i+1)$th level is marked as τ_i or τ_i^{-1}. Any braid-group element is represented as a sequence of over and under crossings [e.g., $\tau_i \tau_{i+1}^{-1}$ in Fig. 1(b)]. τ_i's satisfy the braid relations

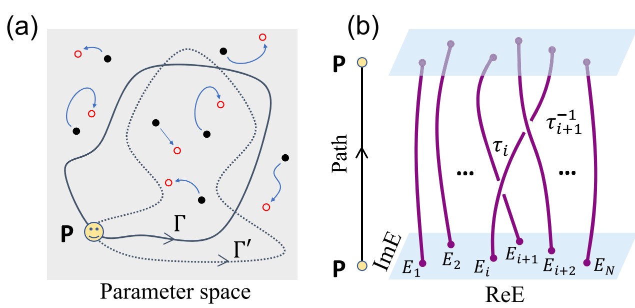

FIG. 1. Schematics of the NACR and braid invariant. (a) Sketch of closed paths based at $\boldsymbol{P}$ (start and end point) enclosing multiple EPs (black dots) in the 2D parameter space. The (black) arrow marks the direction of the path. The analysis equally applies to ELs in the 3D parameter space. Path Γ (solid line) and Γ' (dotted line) are topologically equivalent by smooth deformation. With varying system parameters, the EPs are shifted from their initial positions to final positions (red circles), as marked by blue arrows. (b) An exemplary braiding of eigenenergy strands of an N-band non-Hermitian system along a closed path based at $\boldsymbol{P}$.

$$\begin{cases} \tau_i \tau_j = \tau_j \tau_i, & \text{if } |j-i| > 1; \\ \tau_i \tau_{i+1} \tau_i = \tau_{i+1} \tau_i \tau_{i+1}, & \text{any } 1 \leq i \leq N-1. \end{cases} \tag{2}$$

The homotopy theory [70,71] immediately implies that a smoothly morphing path without touching any EPs or ELs, e.g., $\Gamma \to \Gamma'$ as in Fig. 1(a), yields the same braid invariant. It can be regarded as the NACR for static non-Hermitian Hamiltonians. The flow conservation [72], non-Hermitian doubling theorem [20], and no-go theorem [65] are the special cases of this static NACR [68]. We proceed to consider a time-varying Hamiltonian $H[\lambda(t)]$ with parameter $\boldsymbol{\lambda}$. We investigate the stroboscopic evolution [35,36,48,73–75] of EPs or ELs wherein the nonadiabatic transitions typically encountered in dynamic evolutions can be avoided, and focus on a fixed path Γ in the parameter space, as sketched in Fig. 1(a). It can be shown that as long as no EPs or ELs pass through the path Γ during the whole evolution, the braid invariants at the initial time $b_\Gamma(t_i)$ and final time $b_\Gamma(t_f)$ are conjugate,

$$b_\Gamma(t_f) = b_{dyn}^{-1} b_\Gamma(t_i) b_{dyn}. \tag{3}$$

Here b_{dyn} is purely a dynamical factor describing the accumulated braiding of (instantaneous) eigenenergy from time t_i to t_f at the base point $\boldsymbol{P}$ [68]. As the factor b_{dyn} acts indiscriminately on all the closed paths based at $\boldsymbol{P}$, it would not affect the non-Abelian properties of multiple EPs or ELs. By suitably choosing the base point, we can set $b_{dyn} = 1$. We dub Eq. (3) as a dynamical NACR under parametric evolution. The braid invariant may change during the evolution once extra EPs (ELs) enter or leave the path. As will be seen later, this ostensibly simple rule is powerful in analyzing the collective phenomena of multiple EPs or ELs.

Annihilation and coalescence of EPs.—The non-Abelian exceptional topology brings key nonlocal features in the merging, annihilation, and coalescence process of EPs. As the first application of the NACR, we investigate the merging of two EPs with opposite charges. Figure 2(a) sketches a bizarre case of two EPs (labeled as X and Y) in the parameter space with a time-varying Hamiltonian. Y bypasses another EP (labeled as Z) before rejoining with X. For this case, Z enters and then leaves the closed path Γ during the process. Suppose X and Y were initially created pairwise from a Dirac point or a hybrid EP [34,50,51,68,76–78]. The local braidings of X, Y, Z are denoted as b_X, b_Y, and b_Z, respectively. We have the initial braiding $b_\Gamma(t_i) = b_X b_Y = 1$ and final braiding $b_\Gamma(t_f) = b_X b_Z^{-1} b_X^{-1} b_Z$ [68]. The two EPs do not annihilate each other eventually, except when b_X and b_Z commute, $b_X b_Z = b_Z b_X$. Otherwise, they would coalesce into a higher-order EP. To visualize the difference, we note that the path Γ at t_i and t_f is smoothly deformed to topologically

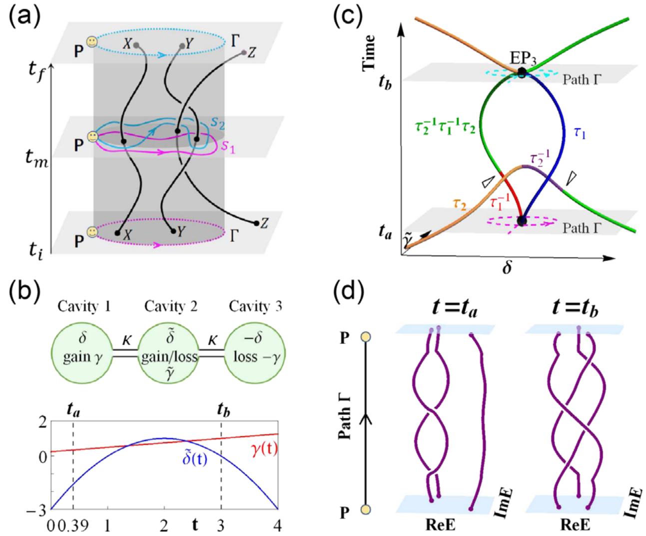

FIG. 2. Annihilation and coalescence of EPs in multiband non-Hermitian systems. (a) Time-evolution loci of the three EP X, Y, Z in the parameter space (black curves). Path Γ at the initial (final) stage is topologically equivalent to s_1 (s_2). (b) (top) Schematics of three coupled acoustic cavities to realize the model (4). κ is the coupling strength. δ, $\tilde{\delta}$ are the detunings. (bottom) Control parameters $\gamma(t)$ and $\tilde{\delta}(t)$ of the protocol as a function of time t. Here $\gamma(t) = (t+1)/4$, $\tilde{\delta}(t) = 1 - (t-2)^2$. (c) EP loci of the model (4) in the 2D $(\delta, \tilde{\gamma})$ space. The EPs are marked by different colors according to their braidings. $t_a \approx 0.39$ and $t_b = 3$ are the time instants when the EP pair emerges and coalesces. The sudden changes of colors are marked by black triangles. (d) The eigenvalue braidings along the path Γ in (c) at $t = t_a$ and $t = t_b$. For (c) and (d) the base point $\boldsymbol{P}$ is pinned at $(\delta, \tilde{\gamma}) = (0, -3)$.

distinct paths s_1 and s_2 at some intermediate time [Fig. 2(a)]. As the noncommutativity occurs between neighboring braidings from the relation in Eq. (2), the annihilation and coalescence exhibit an "adjacent" effect, where an EP pair between the ith and $(i+1)$th bands (with braiding $\tau_i^{\pm 1}$) is unaffected (affected) by its nonadjacent (adjacent) EP (with braiding $\tau_{i\pm 1}^{\pm}$).

Experimental realization.—The path-dependent annihilation of EPs is best illustrated by the following three-state model:

$$H = \begin{pmatrix} \sqrt{2}i[\gamma(t) + i\delta] & -\kappa & 0 \\ -\kappa & i[\tilde{\gamma} + i\tilde{\delta}(t)] & -\kappa \\ 0 & -\kappa & -\sqrt{2}i[\gamma(t) + i\delta] \end{pmatrix}. \tag{4}$$

The model can be readily implemented in various experimental platforms, e.g., coupled acoustic cavities [48–52], as depicted in Fig. 2(b). Here κ is the coupling strength between neighboring cavities. $\kappa = 1$ is set as the energy unit. δ, $\tilde{\delta}(t)$, $-\delta$ are the detunings and $\gamma(t)$, $\tilde{\gamma}$, $-\gamma(t)$ are the gain or loss in the respective cavities. We note that the main physics stays unchanged if only the loss term is present [79,80].

We vary the system parameters as $\gamma(t) = (t+1)/4$ and $\tilde{\delta}(t) = 1 - (t-2)^2$ and examine the evolution of EPs in the 2D $(\delta, \tilde{\gamma})$ space [68]. Figure 2(c) plots the EP loci, with different colors marking their braid-valued invariants [68]. In acoustic cavities, the EP loci can be extracted by measuring the pressure response spectra. Targeted on a pair of EPs created at $t_a \approx 0.39$ with opposite braidings τ_1 and τ_1^{-1}, we observe their subsequent detouring, merging at $t_b = 3$, and splitting for $t > t_b$. Note the abrupt change of braid invariant [marked by the black triangle in Fig. 2(c)] from τ_1^{-1} (red) to $\tau_2^{-1}\tau_1^{-1}\tau_2$ (green) when the EP undercrosses another EP with braiding τ_2 (orange). This is due to the noncommutativity between the braidings τ_1^{-1} and τ_2 [68]. Instead of annihilation, the two initial EPs merge into a third-order EP at $t_b = 3$. Figure 2(d) shows the eigenenergy braidings associated with the path Γ at the two time instants $t = t_a$ (when they are created) and $t = t_b$ (when they coalesce). The braid invariant is 1 (trivial) for the former and $\tau_1\tau_2^{-1}\tau_1^{-1}\tau_2$ for the latter, in agreement with their non-annihilation at $t = t_b$. In experiments, the different properties of the two merging points can be extracted by measuring the eigenspectra nearby or the phase rigidity [49].

Admissible ELs by the conservation rule.—In 3D, the exceptional non-Abelian topology manifests as permissible EL structures compatible with the NACR. To gain intuition, Fig. 3(a) shows two configurations with the red EL component either above or under the blue EL component. Each EL's orientation (arrow) is assigned through the right-hand rule [72]. For the red EL in the left case, the braid invariants at the two ends are the same because the two paths are equivalent by smoothly sliding along the red EL. For the right case, their braid invariants are conjugate by the blue EL: $b_1' = b_2^{-1}b_1b_2$ when the blue EL lies above the red EL [68]. The NACR implies that if the two ELs do not commute $b_1b_2 \neq b_2b_1$, one configuration cannot morph into another: noticing that no EL crosses the two end paths during the deformations (inside the black box), and the braid invariants should stay intact.

Further, two noncommutative ELs cannot form a Hopf link, as depicted in Fig. 3(b). One can check that the braid invariants along the central and faraway paths are not identical. It contradicts the static NACR as the two paths are equivalent. An alternative viewpoint from the dynamical NACR starts from two Weyl points (of a Hermitian system) of two adjacent band gaps separated in the parameter space. By adding gain or loss, two unlinked ELs are spawned from the two Weyl points. The formation of the Hopf link necessitates the illegal crossings in Fig. 3(a). Similarly, we can exclude many other no-go EL structures solely from the NACR without sophisticated model calculations.

We proceed to illustrate a permissible evolution ① → ⑤ as per the NACR [Fig. 3(c)]. The overall process effectively changes EL configurations from a direct crossing to a "tangled" crossing. We take the cavity model (4) yet with a different dynamical protocol:

$$H = \begin{pmatrix} \sqrt{2}i[\gamma(t) - i\delta] & -\kappa & 0 \\ -\kappa & i[-\tilde{\gamma} + i\tilde{\delta}(\beta)] & -\kappa \\ 0 & -\kappa & -\sqrt{2}i[\gamma(t) - i\delta] \end{pmatrix}. \tag{5}$$

We set $\tilde{\delta}(\beta) = 0.3[(\beta - 1)^3 + 3(\beta - 1)^2 - 2]$ $(\beta \in \mathbb{R})$ and slowly vary the parameters $\gamma(t) = t$ to examine the evolution of ELs in the 3D $(\beta, \tilde{\gamma}, \delta)$ space at different time instants [68]. Starting from two noncommutative ELs (red and blue) in ①, we observe their subsequent touching in ②, recombination into staggered rings in ③, and further touching and recombination into tangled ELs in ④⑤. The commutative (noncommutative) components are marked in the same (different) color. In all steps, the braid invariants for the representative path l_1 stay unchanged as required by the NACR. The touching in ② is through higher-order EPs, while in ④, it leads to the reconnection of ELs with adjusted orientations. Unlike the Hopf link in Fig. 3(b), the configuration in ③ has additional EL components at the two wings and is allowed by the NACR. In ③, the first (or third) and second components (counted from left to right) do not commute and cannot be trivially untied. This is verified by the nontrivial braiding of eigenvalue strands in Fig. 3(d) (top panel). The braid invariant for path l_2 at step ①⑤ is obviously trivial. The NACR indicates that the braid invariant for l_2 in step ③ is also trivial, as verified from the trivial braiding of eigenvalue strands in Fig. 3(d) (bottom panel). Thus the second and fourth (or the first and third) components commute (in the same color). We leave detailed model calculations and more interesting examples of admissible ELs to the Supplemental Material [68].

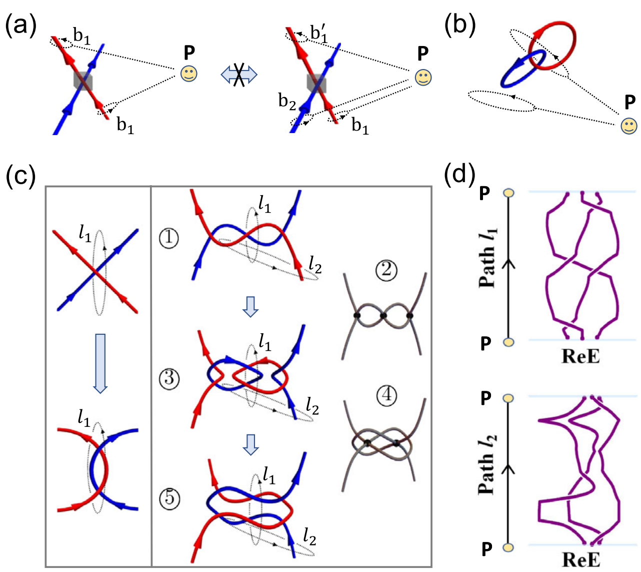

FIG. 3. Admissible exceptional lines (ELs) constrained by the NACR. (a) Two different configurations of ELs (red and blue lines). The dotted lines denote the encircling paths based at P with their braid invariants labeled. (b) Hopf link of noncommutative ELs as a no-go structure. (c) The permissible evolution process of two noncommutative ELs (in red and blue) for model (5). The touchings in step ② are through higher-order EPs (black dots). The braid invariants stay unchanged in all the steps for path l_1 and l_2 as per the NACR. (d) the eigenvalue braidings for path l_1 and l_2 at step ③. The arrows of the ELs in (a)(b)(c) mark the flow.

Discussions.—To conclude, we have demonstrated that the collective behaviors of multiple EPs or ELs in generic multiband non-Hermitian systems are governed by the universal NACR. From this rule, we have uncovered the exotic non-Abelian features of exceptional degeneracies, including the path-dependent annihilation (coalescence) of EPs and the admissible or no-go EL structures. We have further proposed the realizations of these counterintuitive phenomena in acoustic-cavity experiments.

The collective behaviors of multiple EPs or ELs can only be fully captured by the braid invariant which records all the necessary information of non-Abelian topology in multiband non-Hermitian systems. It avoids the oversimplification or ambiguity of the discriminant number or permutation group [52,68,75] (a finite subgroup of B_N). For instance, a closed path enclosing two EPs of the same topological charge (which cannot annihilate) has trivial band permutations. As a bonus, our framework, in an intuitive and exact way, solves the starting-point problem in stroboscopic encircling multiple EPs [81,82]. Different from the homotopy-knot theory of separable bands [62–64], or an isolated EP [65,83] without a base point, the based path is necessary to account for the interplay of multiple EPs. Choosing another base point ends up with a conjugate braid invariant [84]. Yet the non-Abelian physics does not rely on any specific choice.

Applying our results to the 2D or 3D momentum space, the NACR brings distinct non-Abelian features to multiband non-Hermitian metals with exceptional band touchings. It is worth mentioning the key differences from multiband Hermitian topological metals protected by $\mathcal{PT}$ or $\mathcal{C}_2\mathcal{T}$ symmetry described by quaternion charges [85–88] (a finite group). There, the non-Abelian topology is attributed to the frame rotations of wave functions, and there is a definite meaning for band gaps and labeling. (Note the subtlety for Floquet systems [89].) In stark contrast, the complex eigenvalues and defective degeneracies in non-Hermitian settings invalidate a globally consistent numbering of energy bands and band gaps. The non-Abelian topology is encoded in the eigenenergies. Furthermore, the (second-order) EPs (ELs) are defective and stable without symmetry requirements.

Besides acoustic cavities, the illustrated models and phenomena could also be realized and observed in other platforms like coupled optical waveguides [43–47] or ring resonators [37–42]. Besides the EP annihilation (coalescence) and admissible EL structures presented here, the NACR can be utilized to analyze various other collective phenomena, e.g., the exchanges or braidings of EPs or ELs, where the infinite many braid-group elements should give rise to unique non-Abelian properties. Our findings are generic with far-reaching implications in various fields, including optics and photonics to microwaves and acoustics. They should motivate further research on the applications and functionality based on exceptional non-Hermitian physics.

This work is supported by the National Key Research and Development Program of China (Grant No. 2022YFA 1405800), the NSFC under Grants No. 11974413 and No. T2121001, the Strategic Priority Research Program of Chinese Academy of Sciences under Grant No. XDB33 000000, and the start-up Grant of IOP-CAS (H. H.). K. D. is supported by the NSFC under Grant No. 12174072 and Natural Science Foundation of Shanghai (No. 21ZR140 3700).

[*]Corresponding author.
hhu@iphy.ac.cn

[1] M. V. Berry, Physics of non-Hermitian degeneracies, Czech. J. Phys. **54**, 1039 (2004).

[2] W. D. Heiss, The physics of exceptional points, J. Phys. Math. Gen. **45**, 444016 (2012).

[3] M.-A. Miri and A. Alù, Exceptional points in optics and photonics, Science **363**, eaar7709 (2019).

[4] N. Moiseyev, *Non-Hermitian Quantum Mechanics* (Cambridge University Press, Cambridge, England, 2011).

[5] E. J. Bergholtz, J. C. Budich, and F. K. Kunst, Exceptional topology of non-Hermitian systems, Rev. Mod. Phys. **93**, 015005 (2021).

[6] K. Ding, C. Fang, and G. Ma, Non-Hermitian topology and exceptional-point geometries, Nat. Rev. Phys. **4**, 745 (2022).

[7] H. Hodaei, M.-A. Miri, M. Heinrich, D. N. Christodoulides, and M. Khajavikhan, Parity-time–symmetric microring lasers, Science **346**, 975 (2014).

[8] L. Feng, Z. J. Wong, R.-M. Ma, Y. Wang, and X. Zhang, Single-mode laser by parity-time symmetry breaking, Science **346**, 972 (2014).

[9] A. Regensburger, C. Bersch, M.-A. Miri, G. Onishchukov, D. N. Christodoulides, and U. Peschel, Parity-time synthetic photonic lattices, Nature (London) **488**, 167 (2012).

[10] Z. Lin, H. Ramezani, T. Eichelkraut, T. Kottos, H. Cao, and D. N. Christodoulides, Unidirectional Invisibility Induced by PT-Symmetric Periodic Structures, Phys. Rev. Lett. **106**, 213901 (2011).

[11] X. Wang, X. Fang, D. Mao, Y. Jing, and Y. Li, Extremely Asymmetrical Acoustic Metasurface Mirror at the Exceptional Point, Phys. Rev. Lett. **123**, 214302 (2019).

[12] W. Chen, S. K. Özdemir, G. Zhao, J. Wiersig, and L. Yang, Exceptional points enhance sensing in an optical microcavity, Nature (London) **548**, 192 (2017).

[13] M. P. Hokmabadi, A. Schumer, D. N. Christodoulides, and M. Khajavikhan, Non-Hermitian ring laser gyroscopes with enhanced Sagnac sensitivity, Nature (London) **576**, 70 (2019).

[14] H. Hodaei, A. U. Hassan, S. Wittek, H. Garcia-Gracia, R. El-Ganainy, D. N. Christodoulides, and M. Khajavikhan, Enhanced sensitivity at higher-order exceptional points, Nature (London) **548**, 187 (2017).

[15] J. Wiersig, Enhancing the Sensitivity of Frequency and Energy Splitting Detection by Using Exceptional Points: Application to Microcavity Sensors for Single-Particle Detection, Phys. Rev. Lett. **112**, 203901 (2014).

[16] S. Longhi, Quantum interference and exceptional points, Opt. Lett. **43**, 5371 (2018).

[17] W. Cao, X. Lu, X. Meng, J. Sun, H. Shen, and Y. Xiao, Reservoir-Mediated Quantum Correlations in Non-Hermitian Optical System, Phys. Rev. Lett. **124**, 030401 (2020).

[18] F. Roccati, S. Lorenzo, G. Calajò, G. M. Palma, A. Carollo, and F. Ciccarello, Exotic interactions mediated by a non-Hermitian photonic bath, Optica **9**, 565 (2022).

[19] Z. Gong, M. Bello, D. Malz, and F. K. Kunst, Anomalous Behaviors of Quantum Emitters in Non-Hermitian Baths, Phys. Rev. Lett. **129**, 223601 (2022).

[20] Z. Yang, A. Schnyder, J. Hu, and C.-K. Chiu, Fermion Doubling Theorems in Two-Dimensional Non-Hermitian Systems for Fermi Points and Exceptional Points, Phys. Rev. Lett. **126**, 086401 (2021).

[21] Y. Xu, S.-T. Wang, and L.-M. Duan, Weyl Exceptional Rings in a Three-Dimensional Dissipative Cold Atomic Gas, Phys. Rev. Lett. **118**, 045701 (2017).

[22] A. Cerjan, S. Huang, M. Wang, K. P. Chen, Y. Chong, and M. C. Rechtsman, Experimental realization of a Weyl exceptional ring, Nat. Photonics **13**, 623 (2019).

[23] J. Carlström and E. J. Bergholtz, Exceptional links and twisted Fermi ribbons in non-Hermitian systems, Phys. Rev. A **98**, 042114 (2018).

[24] Z. Yang and J. Hu, Non-Hermitian Hopf-link exceptional line semimetals, Phys. Rev. B **99**, 081102(R) (2019).

[25] J. Carlström, M. Stålhammar, J. C. Budich, and E. J. Bergholtz, Knotted non-Hermitian metals, Phys. Rev. B **99**, 161115(R) (2019).

[26] A. Cerjan, M. Xiao, L. Yuan, and S. Fan, Effects of non-Hermitian perturbations on Weyl Hamiltonians with arbitrary topological charges, Phys. Rev. B **97**, 075128 (2018).

[27] M. Stålhammar, L. Rødland, G. Arone, J. C. Budich, and E. J. Bergholtz, Hyperbolic nodal band structures and knot invariants, SciPost Phys. **7**, 019 (2019).

[28] Z. Yang, C.-K. Chiu, C. Fang, and J. Hu, Jones Polynomial and Knot Transitions in Hermitian and non-Hermitian Topological Semimetals, Phys. Rev. Lett. **124**, 186402 (2020).

[29] X. Zhang, G. Li, Y. Liu, T. Tai, R. Thomale, and C. H. Lee, Tidal surface states as fingerprints of non-Hermitian nodal knot metals, Commun. Phys. **4**, 1 (2021).

[30] H. Wang, J. Ruan, and H. Zhang, Non-Hermitian nodal-line semimetals with an anomalous bulk-boundary correspondence, Phys. Rev. B **99**, 075130 (2019).

[31] G. Xu, W. Li, X. Zhou, H. Li, Y. Li, S. Fan, S. Zhang, D. N. Christodoulides, and C.-W. Qiu, Observation of Weyl exceptional rings in thermal diffusion, Proc. Natl. Acad. Sci. U.S.A. **119**, e2110018119 (2022).

[32] D. Leykam, K. Y. Bliokh, C. Huang, Y. D. Chong, and F. Nori, Edge Modes, Degeneracies, and Topological Numbers in Non-Hermitian Systems, Phys. Rev. Lett. **118**, 040401 (2017).

[33] H. Zhou, C. Peng, Y. Yoon, C. W. Hsu, K. A. Nelson, L. Fu, J. D. Joannopoulos, M. Soljačić, and B. Zhen, Observation of bulk Fermi arc and polarization half charge from paired exceptional points, Science **359**, 1009 (2018).

[34] H. Shen, B. Zhen, and L. Fu, Topological Band Theory for Non-Hermitian Hamiltonians, Phys. Rev. Lett. **120**, 146402 (2018).

[35] C. Dembowski, H.-D. Gräf, H. L. Harney, A. Heine, W. D. Heiss, H. Rehfeld, and A. Richter, Experimental Observation of the Topological Structure of Exceptional Points, Phys. Rev. Lett. **86**, 787 (2001).

[36] T. Gao, E. Estrecho, K. Y. Bliokh, T. C. H. Liew, M. D. Fraser, S. Brodbeck, M. Kamp, C. Schneider, S. Höfling, Y. Yamamoto, F. Nori, Y. S. Kivshar, A. G. Truscott, R. G. Dall, and E. A. Ostrovskaya, Observation of non-Hermitian degeneracies in a chaotic exciton-polariton billiard, Nature (London) **526**, 554 (2015).

[37] K. Wang, A. Dutt, K. Y. Yang, C C Wojcik, J. Vučković, and S. Fan, Generating arbitrary topological windings of a non-Hermitian band, Science **371**, 1240 (2021).

[38] K. Wang, A. Dutt, C. C. Wojcik, and S. Fan, Topological complex-energy braiding of non-Hermitian bands, Nature (London) **598**, 59 (2021).

[39] A. Yariv, Y. Xu, R. K. Lee, and A. Scherer, Coupled-resonator optical waveguide: A proposal and analysis, Opt. Lett. **24**, 711 (1999).

[40] M. Hafezi, E. A. Demler, M. D. Lukin, and J. M. Taylor, Robust optical delay lines with topological protection, Nat. Phys. **7**, 907 (2011).

[41] S. Mittal, V. V. Orre, G. Zhu, M. A. Gorlach, A. Poddubny, and M. Hafezi, Photonic quadrupole topological phases, Nat. Photonics **13**, 692 (2019).

[42] H. Zhao, P. Miao, M. H. Teimourpour, S. Malzard, R. El-Ganainy, H. Schomerus, and L. Feng, Topological hybrid silicon microlasers, Nat. Commun. **9**, 981 (2018).

[43] N. X. A. Rivolta and B. Maes, Symmetry recovery for coupled photonic modes with transversal PT symmetry, Opt. Lett. **40**, 3922 (2015).

[44] A. Guo, G. J. Salamo, D. Duchesne, R. Morandotti, M. Volatier-Ravat, V. Aimez, G. A. Siviloglou, and D. N. Christodoulides, Observation of PT-Symmetry Breaking in Complex Optical Potentials, Phys. Rev. Lett. **103**, 093902 (2009).

[45] L. Feng, Y.-L. Xu, W. S. Fegadolli, M.-H. Lu, J. E. B. Oliveira, V. R. Almeida, Y.-F. Chen, and A. Scherer, Experimental demonstration of a unidirectional reflectionless parity-time metamaterial at optical frequencies, Nat. Mater. **12**, 108 (2013).

[46] X.-L. Zhang, S. Wang, B. Hou, and C. T. Chan, Dynamically Encircling Exceptional Points: In situ Control of Encircling Loops and the Role of the Starting Point, Phys. Rev. X **8**, 021066 (2018).

[47] J. Doppler, A. A. Mailybaev, J. Böhm, U. Kuhl, A. Girschik, F. Libisch, T. J. Milburn, P. Rabl, N. Moiseyev, and S. Rotter, Dynamically encircling an exceptional point for asymmetric mode switching, Nature (London) **537**, 76 (2016).

[48] K. Ding, G. Ma, M. Xiao, Z. Q. Zhang, and C. T. Chan, Emergence, Coalescence, and Topological Properties of Multiple Exceptional Points and Their Experimental Realization, Phys. Rev. X **6**, 021007 (2016).

[49] W. Tang, X. Jiang, K. Ding, Y.-X. Xiao, Z.-Q. Zhang, C. T. Chan, and G. Ma, Exceptional nexus with a hybrid topological invariant, Science **370**, 1077 (2020).

[50] K. Ding, G. Ma, Z. Q. Zhang, and C. T. Chan, Experimental Demonstration of an Anisotropic Exceptional Point, Phys. Rev. Lett. **121**, 085702 (2018).

[51] W. Tang, K. Ding, and G. Ma, Direct Measurement of Topological Properties of an Exceptional Parabola, Phys. Rev. Lett. **127**, 034301 (2021).

[52] W. Tang, K. Ding, and G. Ma, Experimental realization of non-Abelian permutations in a three-state non-Hermitian system, Natl. Sci. Rev. **9**, nwac010 (2022).

[53] L. Xiao, T. Deng, K. Wang, Z. Wang, W. Yi, and P. Xue, Observation of Non-Bloch Parity-Time Symmetry and Exceptional Points, Phys. Rev. Lett. **126**, 230402 (2021).

[54] K. Wang, L. Xiao, J. C. Budich, W. Yi, and P. Xue, Simulating Exceptional Non-Hermitian Metals with Single-Photon Interferometry, Phys. Rev. Lett. **127**, 026404 (2021).

[55] C. Zhong, Y. Chen, Z.-M. Yu, Y. Xie, H. Wang, S. A. Yang, and S. Zhang, Three-dimensional Pentagon Carbon with a genesis of emergent fermions, Nat. Commun. **8**, 15641 (2017).

[56] Z. Yan, R. Bi, H. Shen, L. Lu, S.-C. Zhang, and Z. Wang, Nodal-link semimetals, Phys. Rev. B **96**, 041103(R) (2017).

[57] R. Bi, Z. Yan, L. Lu, and Z. Wang, Nodal-knot semimetals, Phys. Rev. B **96**, 201305(R) (2017).

[58] M. Ezawa, Topological semimetals carrying arbitrary Hopf numbers: Fermi surface topologies of a Hopf link, Solomon's knot, trefoil knot, and other linked nodal varieties, Phys. Rev. B **96**, 041202(R) (2017).

[59] W. Chen, H.-Z. Lu, and J.-M. Hou, Topological semimetals with a double-helix nodal link, Phys. Rev. B **96**, 041102(R) (2017).

[60] Y. Zhou, F. Xiong, X. Wan, and J. An, Hopf-link topological nodal-loop semimetals, Phys. Rev. B **97**, 155140 (2018).

[61] C. H. Lee, A. Sutrisno, T. Hofmann, T. Helbig, Y. Liu, Y. S. Ang, L. K. Ang, X. Zhang, M. Greiter, and R. Thomale, Imaging nodal knots in momentum space through topolectrical circuits, Nat. Commun. **11**, 4385 (2020).

[62] C. C. Wojcik, X.-Q. Sun, T. Bzdušek, and S. Fan, Homotopy characterization of non-Hermitian Hamiltonians, Phys. Rev. B **101**, 205417 (2020).

[63] Z. Li and R. S. K. Mong, Homotopical classification of non-Hermitian band structures, Phys. Rev. B **103**, 155129 (2021).

[64] H. Hu and E. Zhao, Knots and Non-Hermitian Bloch Bands, Phys. Rev. Lett. **126**, 010401 (2021).

[65] H. Hu, S. Sun, and S. Chen, Knot topology of exceptional point and non-Hermitian no-go theorem, Phys. Rev. Res. **4**, L022064 (2022).

[66] C. C. Wojcik, K. Wang, A. Dutt, J. Zhong, and S. Fan, Eigenvalue topology of non-Hermitian band structures in two and three dimensions, Phys. Rev. B **106**, L161401 (2022).

[67] T. Bzdušek and M. Sigrist, Robust doubly charged nodal lines and nodal surfaces in centrosymmetric systems, Phys. Rev. B **96**, 155105 (2017).

[68] See Supplemental Material at http://link.aps.org/supplemental/10.1103/PhysRevLett.130.157201 for details on (I) the derivation of the homotopy invariants for closed paths in the parameter space; (II) the relation between the conservation rule and other theorems; (III) the proof of the dynamical non-Abelian conservation rule; (IV) the merging of EPs in the two-band case; (V) the derivation of braid invariants at initial and final stages; (VI) theoretical design of model parameters; (VII) the derivation of the EP trajectories for model Eq. (4); (VIII) the conjugate relation; (IX) the model realizations of various EL configurations of Fig. 3 in acoustic cavities; (X) the example of the EL emergence allowed by the conservation rule; (XI) comparison between different topological invariants, which includes Ref. [69].

[69] D. C Brody, Biorthorgonal quantum mechanics, J. Phys. A **47**, 035305 (2014).

[70] N. D. Mermin, The topological theory of defects in ordered media, Rev. Mod. Phys. **51**, 591 (1979).

[71] J. C. Y. Teo and T. L. Hughes, Topological defects in symmetry-protected topological phases, Annu. Rev. Condens. Matter Phys. **8**, 211 (2017).

[72] X. Cui, R.-Y. Zhang, W.-J. Chen, Z.-Q. Zhang, and C. T. Chan, Symmetry-protected topological exceptional chains in non-Hermitian crystals, arXiv:2204.08052.

[73] W. D. Heiss and G. Wunner, Chiral behaviour of the wave functions for three wave guides in the vicinity of an exceptional point of third order, Eur. Phys. J. D **71**, 312 (2017).

[74] J.-W. Ryu, S.-Y. Lee, and S. W. Kim, Analysis of multiple exceptional points related to three interacting eigenmodes in a non-Hermitian Hamiltonian, Phys. Rev. A **85**, 042101 (2012).

[75] Q. Zhong, M. Khajavikhan, D. N. Christodoulides, and R. El-Ganainy, Winding around non-Hermitian singularities, Nat. Commun. **9**, 4808 (2018).

[76] O. N. Kirillov, A. A. Mailybaev, and A. P. Seyranian, Unfolding of eigenvalue surfaces near a diabolic point due to a complex perturbation, J. Phys. A **38**, 5531 (2005).

[77] A. P. Seyranian, O. N. Kirillov, and A. A. Mailybaev, Coupling of eigenvalues of complex matrices at diabolic and exceptional points, J. Phys. A **38**, 1723 (2005).

[78] Y.-X. Xiao, Z.-Q. Zhang, Z. H. Hang, and C. T. Chan, Anisotropic exceptional points of arbitrary order, Phys. Rev. B **99**, 241403(R) (2019).

[79] M. Ornigotti1 and A. Szameit1, Quasi $\mathcal{PT}$-symmetry in passive photonic lattices, J. Opt. **16**, 065501 (2014).

[80] Y. N. Joglekar and A. K. Harter, Passive parity-time-symmetry-breaking transitions without exceptional points in dissipative photonic systems [Invited], Photonics Res. **6**, A51 (2018).

[81] E. J. Pap, D. Boer, and H. Waalkens, Non-Abelian nature of systems with multiple exceptional points, Phys. Rev. A **98**, 023818 (2018).

[82] J.-W. Ryu, S.-Y. Lee, and S. W. Kim, Analysis of multiple exceptional points related to three interacting eigenmodes in a non-Hermitian Hamiltonian, Phys. Rev. A **85**, 042101 (2012).

[83] Y. S. S. Patil, J. Höller, P. A. Henry, C. Guria, Y. Zhang, L. Jiang, N. Kralj, N. Read, and J. G. E. Harris, Measuring the knot of non-Hermitian degeneracies and non-commuting braids, Nature (London) **607**, 271 (2022).

[84] A. Hatcher, *Algebraic Topology* (Cambridge University Press, Cambridge, England, 2002).

[85] Q. S. Wu, A. A. Soluyanov, and T. Bzdušek, Non-Abelian band topology in noninteracting metals, Science **365**, 1273 (2019).

[86] A. Bouhon, Q. S. Wu, R.-J. Slager, H. Weng, O. V. Yazyev, and T. Bzdušek, Non-Abelian reciprocal braiding of Weyl points and its manifestation in ZrTe, Nat. Phys. **16**, 1137 (2020).

[87] A. Tiwari and T. Bzdušek, Non-Abelian topology of nodal-line rings in PT-symmetric systems, Phys. Rev. B **101**, 195130 (2020).

[88] A. Bouhon, T. Bzdušek, and R.-J. Slager, Geometric approach to fragile topology beyond symmetry indicators, Phys. Rev. B **102**, 115135 (2020).

[89] R.-J. Slager, A. Bouhon, and F. Nur. Ünal, Floquet multi-gap topology: Non-Abelian braiding and anomalous Dirac string phase, arXiv:2208.12824.